Plant-derived benzoxazinoids act as antibiotics and shape bacterial communities

Niklas Schandry[1,2,*], Katharina Jandrasits[1], Ruben Garrido-Oter[3], Claude Becker[1,2,*]

[1] Gregor Mendel Institute of Molecular Plant Biology, Austrian Academy of Sciences, Vienna BioCenter (VBC), 1030 Vienna, Austria
[2] Genetics, Faculty of Biology, Ludwig Maximilians University Munich, 82152 Martinsried, Germany
[3] Department of Plant Microbe Interactions, Max Planck Institute for Plant Breeding Research, 50829 Cologne, Germany

* Correspondence should be addressed to claude.becker@bio.lmu.de and niklas.schandry@bio.lmu.de

Abstract

Plants synthesize and release specialized metabolites into their environment that can serve as chemical cues for other organisms. Metabolites that are released from the roots are important factors in determining which microorganisms will colonize the root and become part of the plant rhizosphere microbiota. Root exudates are often further converted by soil microorganisms, which can result in the formation of toxic compounds. How individual members of the plant rhizosphere respond to individual compounds and how the differential response of individual microorganisms contributes to the response of a microbial community remains unclear. Here, we investigated the impact of derivatives of one class of plant root exudates, benzoxazinoids, which are released by important crops such as wheat and maize, on a collection of 180 root-associated bacteria. We show that phenoxazine, derived from benzoxazinoids, inhibits the growth of root-associated bacteria *in vitro* in a strain-specific manner, with sensitive and resistant isolates in most of the studied clades. Synthetic bacterial communities that were assembled from only resistant isolates were more resilient to chemical perturbations than communities comprised of only sensitive members. Isolates that were shared between different communities showed stable interactions, independent of the overall community composition. On the other hand, we could attribute differential community development to differences in interactions formed by closely related representatives of the same bacterial genus. Our findings highlight the fact that profiling isolate collections can aid the rational design of synthetic communities. Moreover, our data show that simplified *in vitro* community systems are able to recapitulate observations on the influence of metabolite exudation on the structure of root-associated communities, thus providing an avenue for reductionist explorations of the rhizosphere biology in defined, host-free settings.

Introduction

In the rhizosphere, the space directly surrounding the roots, plants recruit and maintain a diverse community of microorganisms that differs from the surrounding bulk soil [1–4]. These rhizospheric microbiota, in particular bacteria and fungi, contribute to plant nutrition, growth, and defense [1].

While it is clear that there are biochemical interactions at play in the establishment and the qualitative and quantitative modulation of the microbiota, the chemical ecology of the rhizosphere is not well understood, in part owing to the biological, chemical, and physical complexity of the soil environment. Recent studies have shown, however, that some plant specialized metabolites contribute to plant species-specific community profiles in the rhizosphere. For example, salicylic acid, camalexin, coumarins, and glucosinolates play an important role in shaping the *Arabidopsis thaliana* rhizosphere [4–9].

Members of the Poaceae family (grasses), including wheat and maize, produce a particular class of specialized metabolites, the benzoxazinoids (BX) [10, 11]. Chemically, BX and some of their breakdown products chelate trivalent ions and have been suggested to act as phytosiderophores in iron uptake or as protective ion scavengers [12]. BX and their derivatives

affect different branches of the tree of life: they act as herbivore repellents when stored in plant leaves, can be hijacked by nematodes to deter predators, or interfere with the growth of nearby plants [13–16]. Beyond acting on these larger-sized eukaryotes, BX exert a major influence on root-associated fungal and bacterial microbiota. For example, BX exudation by maize plants into the surrounding soil leads to conditioning of the microbiome, which in turn results in soil-memory effects that affect plants of the following sowing [17]. Another study showed that BX exudation specifically recruits beneficial pseudomonads to the rhizosphere [18–22].

Conversely, the presence and composition of the microbiota can alter BX chemistry. Post-release breakdown and metabolism of benzoxazinoid compounds by soil microbiota leads to the sequential formation of 1,4-benzoxazin-3-one (BOA) and 2-amino-3-phenoxazinone (APO), among other compounds, in non-sterile soils [23–25]. APO in return exhibits antibiotic activity similar to other phenoxazines and limits plant root growth at concentrations corresponding to those detected in soil [14, 15, 26–28].

To date, the selectivity and antimicrobial activity of BX and their non-benzoxazinoid derivatives such as APO on soil-dwelling and root-associated bacteria has not been systematically addressed, and it remains elusive how bacterial communities respond to these compounds. Given the long-term microbiome-conditioning capacity of BX exudation described above [17], it is tempting to speculate that some of the plant-growth-inhibitory effects of BX compounds could be mediated by selective effects on the plant-associated microbiota [29]. However, quantitative analyses of the degree to which microbial isolates differ in their response to root exudates are extremely difficult to perform in soil, because (*i*) plant-associated microbiota are highly diverse, and (*ii*) plant exudates are typically complex mixtures, making it difficult to attribute effects to a particular chemical. In contrast, such studies can be easily carried out *in vitro* using clonal bacterial populations (strains) and pure compounds at defined concentrations.

Collections of culturable bacterial isolates from diverse habitats are an important resource to investigate how diverse microorganisms respond to biotic and abiotic environmental cues or to chemical exposure (e.g. antibiotics, toxins, or pollutants). Such collections can moreover form the basis for rationally designed synthetic microbial communities (syncoms) [30, 31]. Syncoms have been proposed and used as reduced complexity systems to study how various microbiomes assemble and develop over time [7, 32–35]. In these studies, the function of individual members has emerged as a key predictor of community function, whereas taxonomic composition appears to be less crucial. Syncoms have gained traction as simplified models for naturally occurring communities and are an emerging tool for the targeted modulation of plant health, through holobiont (the organism formed by host and microbiome) design [36]. Bacterial syncoms in particular have been adopted in plant sciences to study various aspects of plant biology, including plant phenotypes under limiting phosphate conditions [31], assembly of the phyllosphere microbiome [37, 38], or assembly cues of the root microbiome [7, 34, 39]. Syncoms assembled from plant-associated bacteria have not yet been studied for their ability to assemble stable communities *in vitro* in the absence of a host, although such a system would significantly reduce the experimental complexity. Such *in vitro* systems have already been adopted in other systems, for example for gut microbiota research [40].

The assembly of a community from individual strains is a complex process involving basic metabolic (competitive or mutualistic) and chemical interactions between the different members that form the community. In addition, environmental perturbations may destabilize a community,

shift its composition, or affect which individuals can establish themselves. The stability of rhizospheric communities towards environmental perturbations is an important aspect of rhizosphere biology. With the advent of precision agriculture and highly controlled growth environments, engineering of the rhizosphere is an emerging topic that encompasses plant biology, microbiology, microbial ecology, as well as genetic and biochemical biological disciplines [41, 42].

Here, we investigated the impact of BX and their derivatives on bacterial members of the plant root and rhizosphere. We used the *AtRSphere* collection, derived from the root and rhizosphere of the model plant species *Arabidopsis thaliana* that includes around 180 culturable isolates distributed across four bacterial phyla [39] for dose-dependent *in vitro* responses to the BX APO and BOA, which can be found in soil surrounding BX-releasing plants.

A. thaliana is not a BX producer, therefore the ability of a strain to colonize *A. thaliana* roots should be independent of its BX tolerance. In line with this assumption, our study revealed a wide range of growth responses, particularly to APO, among the *A. thaliana* derived *AtRSphere* collection. This occurred both within and across genera, ranging from complete insensitivity to strongly impacted growth. Information on the individual strains' response guided our design of syncoms to investigate how BX and BX derivatives shape community assembly *in vitro.* We made use of the strain-level diversity we observed in the collection with regards to BX exposure, to explore their potential to form communities differing in resilience to BX-mediated community perturbations. We found that the ability of a strain to establish as a community member is often uncorrelated to growth in pure culture, and that sensitivity of a strain to BX may change unpredictably when embedded in a community. Nevertheless, we also found that syncoms underwent compositional changes *in vitro* that reflected those previously observed in soil. Since the included isolates partially overlapped between generated syncoms, we conducted a comparative analysis to understand how chemical treatment and identity of member strains shape the composition of *in vitro* communities.

Results

BX derivatives selectively inhibit the growth of root associated bacteria *in vitro*

To gain an overview of how benzoxazinoids and their derivatives affect individual plant-associated bacteria, we screened the *AtRSphere* collection comprising 180 isolates of *A. thaliana* rhizospheric bacteria [39] (Figure 1). We monitored the growth of each strain over 70 h in half-strength TSB medium after supplementation with either BOA (Figure 1A, inner heatmap) or APO (Figure 1A, outer heatmap), two plant-BX-derived compounds commonly found in soil, and under control conditions (equivalent concentration of solvent only). By determining cell density at regular intervals, we assessed each isolate’s response to different compound concentrations.

The growth of most isolates was not inhibited by BOA, even at high concentrations of 100 µM. Some isolates even seemed to benefit (darker color in Figure 1) from the presence of BOA

compared with control conditions; this was most consistent for isolates within the *Rhizobium* and *Paenibacillus* genera (Figure 1B, C). However, such growth promotion was rare overall. This might be attributable to the use of a nutrient-rich medium in this study, which would make BOA superfluous as a potential energy source.

In stark contrast to the overall weak impact of BOA, exposure to APO severely inhibited growth of 43% of the isolates (77/180 isolates grew to less than 50% of control levels in 50 μM APO) (Figure 1A). Some isolates were insensitive to low APO concentrations but showed growth inhibition at concentrations ≥10 μM, while others showed inhibition already at 5 μM APO (Figure 1). Generally, the impact of APO on growth was dose dependent. Overall, sensitivity to APO appeared to be isolate-specific, as sensitivities varied as widely within as they did across families and genera. APO-sensitive strains (defined as showing <50% relative growth at 50 μM APO) were present in all families covered by the *AtRSphere* collection (Figure 1A), with the exception of the *Pseudomonadaceae* and *Alcaligenaceae* (Figure 1D, E). Within those clades that contained APO-sensitive isolates, the response pattern did not follow an obvious phylogenetic structure (16S rRNA-based phylogeny), indicating that sensitivity to APO is species- or even strain-specific within one genus.

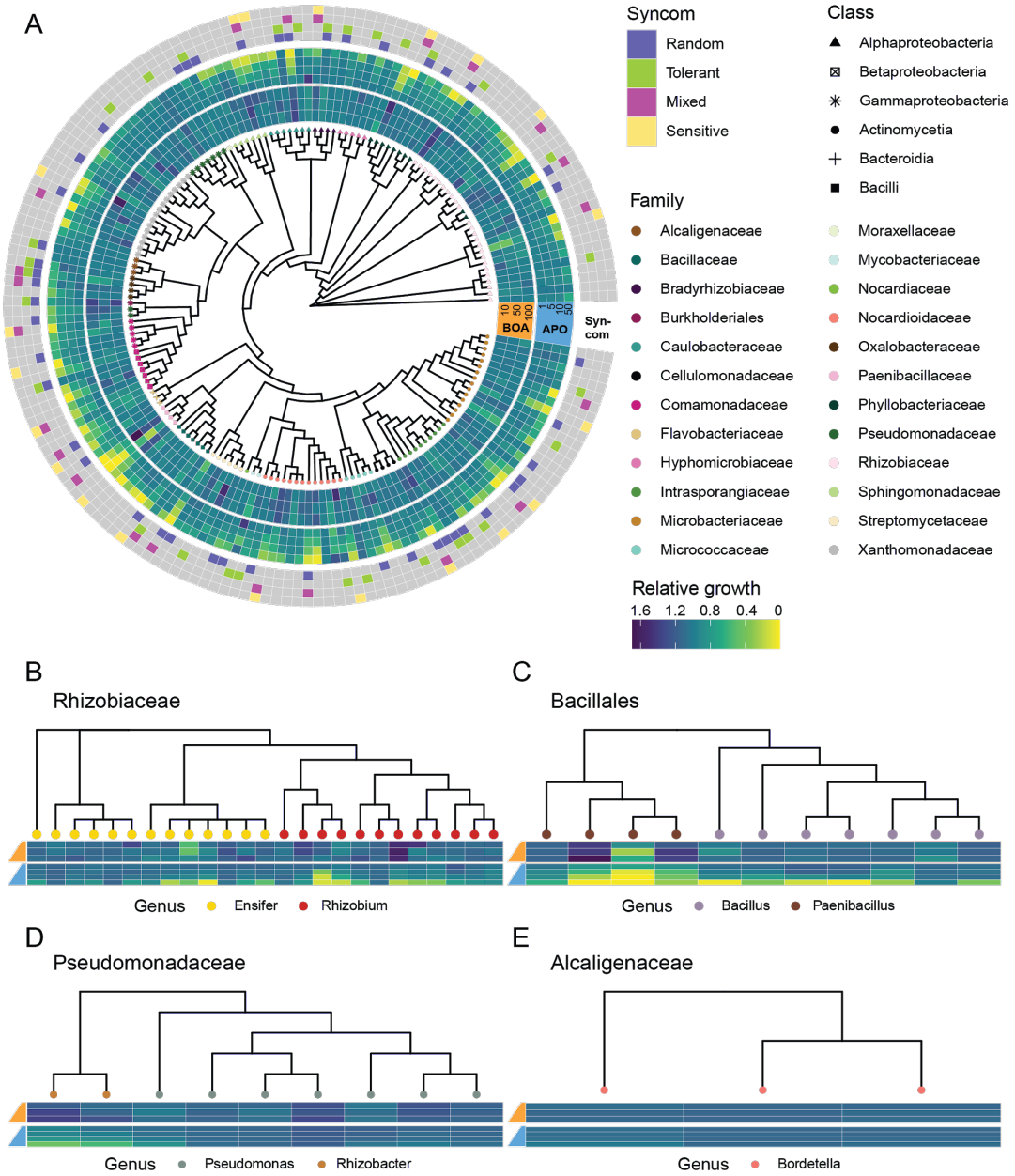

Figure 1. Isolate sensitivity to BX compounds and derivatives.
A) Heatmap arranged around a circular phylogenetic tree computed from 16S rRNA sequences. Nodes represent isolates from the collection, node shape indicates taxonomic class, node color indicates taxonomic family. The inner heatmap displays average relative growth when treated with BOA (from inner to outer: 10 μM, 50 μM and 100 μM BOA, rings 1-3). The central heatmap displays relative growth upon APO treatment (inner to outer: 1 μM, 5 μM, 10 μM and 50 μM, rings 4-7). The outer heatmap indicates whether or not the isolate was selected as a member of one of the 4 synthetic communities (see main text for details).
B-E) Sub-tree of isolates from the Rhizobiaceae family (B), Bacillales order (C), Pseudomonadaceae family (D), and Alcaligenaceae family (E); the heatmap displays relative growth in BOA (Orange, from top to bottom: 10 μM, 50 μM, 100 μM) and APO (Blue, from top to bottom: 1 μM, 5 μM, 10 μM and 50 μM). Node color represents taxonomic assignment at the genus level (legend below the heatmap).

Synthetic bacterial communities are structured by BX treatment

Since we were interested in the effect of BX on communities, we designed four different syncoms based on the responses of the individual isolates: one that fully represented the isolate collection at the genus level by randomly choosing one isolate per genus (referred to hereafter as *random*) and three reduced-complexity syncoms (Table S1). Of these, the *tolerant* syncom only contained isolates (max. one per genus) that had grown to at least 75% of the control level in 50 µM APO. As can be seen in Figure 1A, several isolates that were part of *tolerant* were also included in *random* (Figure 1A). The *sensitive* syncom consisted only of isolates that had grown to less than 25% of control levels in 50 µM APO. Finally, the *mixed* syncom contained both APO-sensitive and APO-tolerant strains (Figure 1A). To understand the temporal and treatment-specific community dynamics, we grew each syncom in three different environments: control (supplemented with DMSO, the solvent used in the other two treatments), 100 µM BOA, and 50 µM APO. We monitored syncom composition in 24 h intervals over 4 d via 16S rRNA sequencing. Amplicon sequence variants (ASVs) were reconstructed from the short reads and assigned to isolates using syncom-specific lookup files.

As all bacteria analyzed here had originally been isolated from complex plant root microbiomes, we first assessed to which degree they could reassemble into communities *in vitro* in the absence of a host. Principal coordinate analysis (PCoA) of Jaccard distances calculated from relative abundances revealed that syncoms assembled reproducibly (Figure 2A-D)

We next assessed if communities containing only APO-sensitive isolates would be more strongly restructured by the addition of APO than one assembled only from APO-tolerant isolates. We again used the Jaccard distance to measure within-community beta diversity and performed an unconstrained PCoA for each syncom (Figure 2 A-D). Generally, we observed treatment-specific changes in all syncoms. Overall, BOA-treated samples were similar to the control in all syncoms, with the exception of the *sensitive* one. APO-treated samples clustered separately from both control and BOA (Figure 2 A-D). The separation between APO and the remaining samples in the ordination was most obvious for the *mixed* and *random* and less striking for the *tolerant* syncom; it decreased over time in the *sensitive* one (Figure 2A-D).

We performed permutational multivariate analysis of variance (PERMANOVA) to see if we could corroborate these observations. Treatment explained a significant proportion of variance in all syncoms: 40% in *random*, 22% in *tolerant*, 75% in *mixed*, and 41% in *sensitive*. This means that the proportion of between-sample variance explained by BX treatment was lowest in the community assembled from APO-tolerant isolates. In other words, the syncom composed of only the most APO-tolerant individual strains showed the highest resilience to APO. Time point explained a significant proportion of variance in *random* and *tolerant* (31% and 33%, respectively) but not in *mixed* or *sensitive* (Supplemental Table 2).

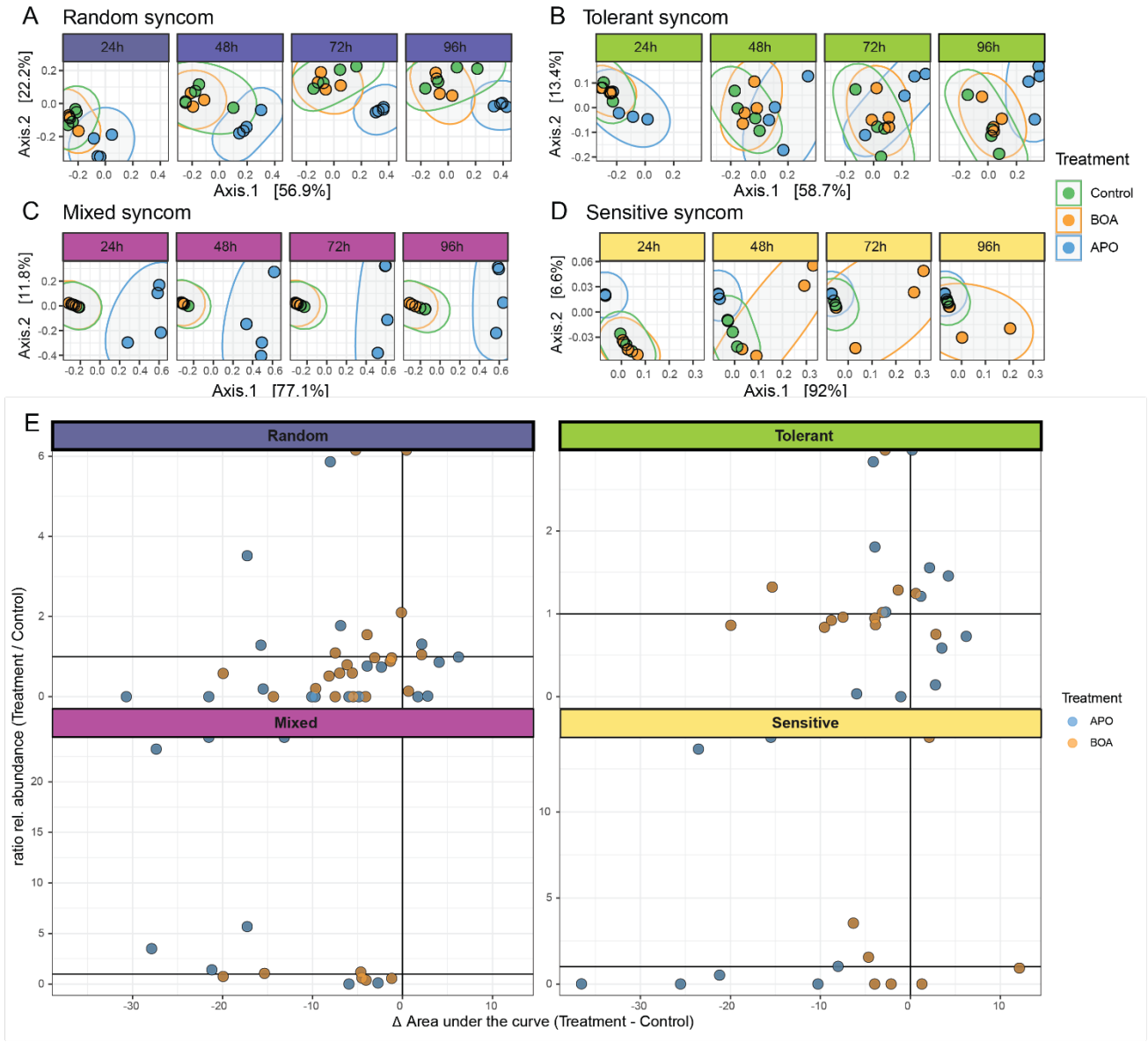

Figure 2. Community analysis.
Principal coordinate analysis (PCoA) of the Jaccard distances computed on relative genus abundances for all samples. A-D) PCoA per syncom; faceted by time point (columns) and colored by treatment. E) Relationship between change in bacterial growth in the presence of BX compounds in pure culture (x-axis) plotted against the change in relative abundance when embedded in a community (y-axis) for APO and BOA. Each dot shows the average change in relative abundance for one isolate across all timepoints.

Having confirmed that the different strain mixtures reliably assembled into reproducible communities, we asked if within-sample species diversity (alpha-diversity) was affected by time or treatment. Overall, there was no clear relationship between the growth of an isolate *in vitro* and the ability of an isolate to establish itself as a syncom member. In fact, some isolates that barely grew when cultured individually reached relative abundances of >90% when grown in a community (Figure 2E).

In the *random*, *tolerant*, and *mixed* syncoms, APO (but not BOA) treatment significantly reduced the total number of taxa at one or more time points, while in the *sensitive* syncom, the taxon

number remained constant across treatments and time points (Figure S1, Supplemental tables S3 and S4). However, while the total number of taxa remained the same, different taxa were driven to extinction (ratio of 0 on the relative abundance scale axis, Figure 2E) by the individual treatments, while the presence of other taxa was specific for one of the compounds (appearing at the very top of each panel in Figure 2E). Time alone, however, did not significantly influence the species number in any of the syncoms. The Shannon measure of alpha diversity, which in addition to the number of species also incorporates the evenness of species abundances, was significantly influenced by both time and treatment (Figure S2, Supplemental Table S5). While APO treatment significantly increased Shannon diversity of the *mixed* and *tolerant* communities, it decreased Shannon diversity of the *sensitive* one. In contrast, BOA significantly increased Shannon diversity of the *sensitive* syncom after 48 h (Supplemental Table S6).

Response of community-embedded isolates to BX treatment

Since previous studies reported a substantial impact of plant-derived BX on soil microbiota [17-20, 22], we were interested in assessing if the reported effects could be recapitulated using reduced complexity communities *in vitro*. To understand which taxa drove the observed differences between treatments, and if similar changes occurred upon APO treatment in the different communities, we estimated the fold-change in taxon abundance per syncom and time point between APO- and BOA-treated samples as well as between APO and control, and between BOA and control (Figure 3). In this first approach, we focused on those taxa that showed a significant fold-change between two treatments for at least one time point.
Overall, we observed APO-dependent shifts in relative abundance of different genera in all syncoms, the comparison of relative abundances between BOA and control conditions only yielded significant differences in the *sensitive* community.
Some genera were consistently reduced in APO-treated communities. These were *Bacillus* in *random* (Figure 3A)*, tolerant* (Figure 3B) and *sensitive* (Figure 3D), *Flavobacterium* in *random* (Figure 3A) and *mixed* (Figure 3C) and *Acidovorax* in every syncom, irrespective of the particular strain used (Fig 3A-D). Other genera thrived in APO-treated samples: *Lysobacter (*in *mixed* and *sensitive*) and *Hoeflea* (identical isolate Root268 in *random* and *sensitive*)*.* Only the genus *Microbacterium* displayed opposing behavior between syncoms: abundance was increased when treated with APO in *mixed* and *sensitive*, while abundance in the *tolerant* community was significant reduced in APO-treated samples at 48h. While *Microbacterium* was significantly reduced in *tolerant* after 48h (see confidence intervals in Fig 3B), it is possible that this is attributable to measurement error, considering that this isolate was only lowly abundant in this community.

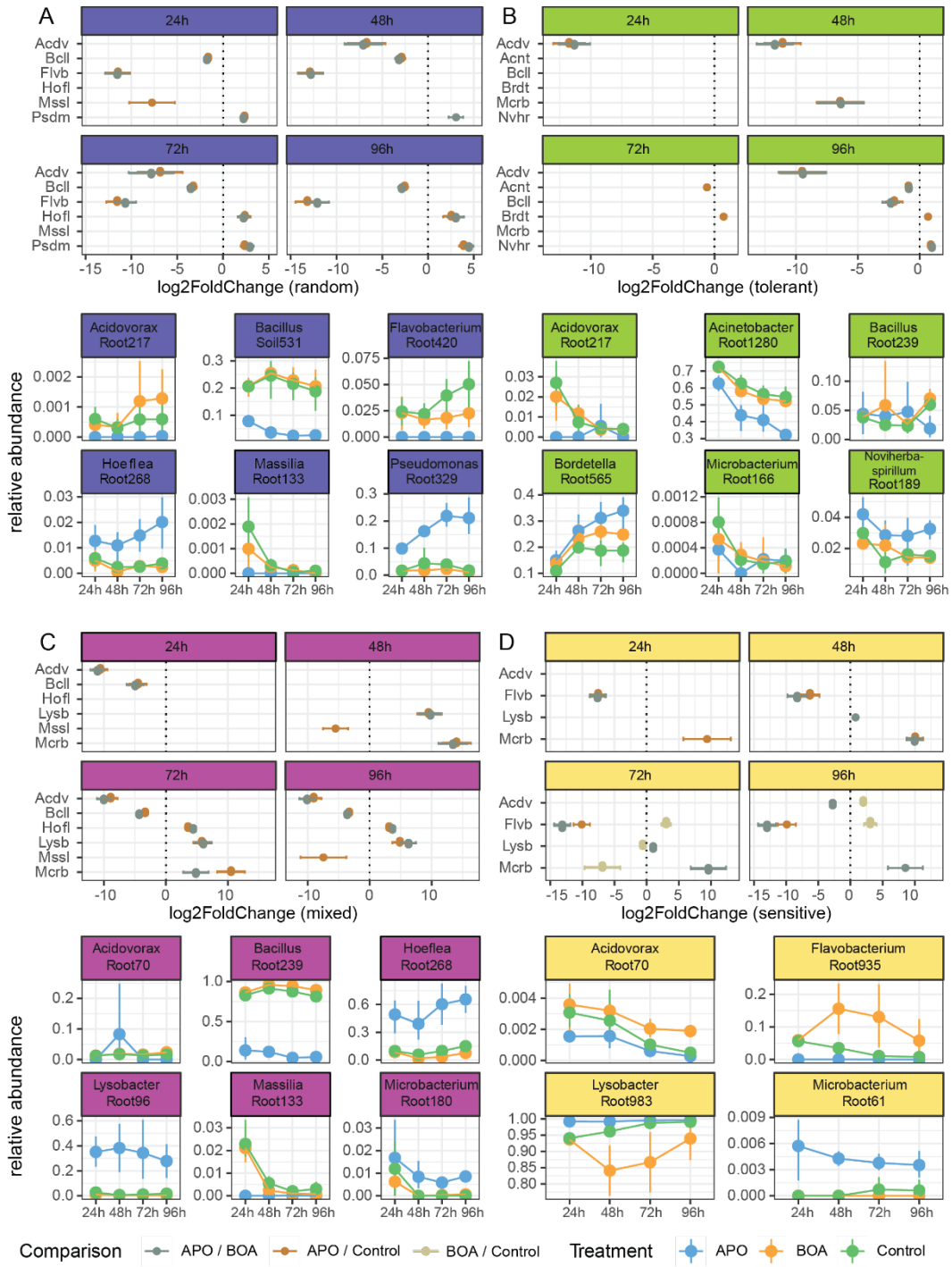

Figure 3. Treatment-specific and temporal strain abundances in syncoms.
Fold-changes between treatments and relative abundances of strains that were significantly different for at least one time point, estimated by DESeq2. Plots are divided by syncom: *random* **(A)**, *tolerant* **(B)**, *mixed* **(C)**, and *sensitive* **(D)**. In fold-change plots (top) only significant changes are shown for each time point. Line graphs (below) show relative abundance for all time points for isolates with significant fold-changes. Dots mark the mean across replicates, error bars indicate the 95% confidence interval.

Interactions between isolates are modulated by community members and chemical treatment

In the next approach, we wanted to move beyond comparing only treatment-specific effects and investigate whether interactions between community members were influenced by community context and chemical treatment. The assignment of isolates to the *random* community had been done blindly. However, the PCoA in Figure 2A already indicated that the *random* and *tolerant* syncoms were the most similar. We attributed this to the fact that the *Acinetobacter*, *Acidovorax*, *Bordetella*, *Massilia*, and *Noviherbaspirillum* isolates were shared between the *random* and *tolerant* syncoms and established themselves in both communities. We also observed that the BOA and APO treatments had community-specific effects on some of those shared isolates (Figure 4A). We therefore reasoned that differences in the relative abundance of these isolates between the two syncoms likely resulted from interactions with other, non-shared syncom members. To test this hypothesis, we calculated Pearson's correlation between sequence counts assigned to isolates in each syncom at 24 h and 96 h. We then constructed correlation networks per treatment and time point, including all correlations with an absolute $r > 0.5$. The networks for BOA and APO at the 24 h and 96 h time points are shown in Figure 4B, the remaining networks in Figure S3.

The *random* and *tolerant* communities became more similar over time when treated with APO, overlapping in 5 genera (out of a total 8) included in the network, confirming the observation in Figure 2A. *Hoeflea* and *Rhodanobacter* were detectable only in the *random* syncom, *Rhizobium* only in the *tolerant* syncom. Some of the shared isolates were not detectable in APO but only in BOA and control conditions: *Massilia* Root133 was detected in the early time point, *Acidovorax* Root217 established itself at the late time point (Figure 4B).

When looking at the interactions between isolates, we observed that after treatment with APO, *Bordetella* Root565, *Noviherbaspirillum* Root189, and *Acinetobacter* Root1280 displayed strong, positive correlations after 96 h in both *tolerant* and *random* syncoms. This suggested that this group of strains engaged in similar interactions, irrespective of the other strains in the community. However, the relative abundance *Acinetobacter* Root1280 appeared to be more affected by APO treatment in the *tolerant* than in the *random* community (Figure 4A). Based on the correlation networks, we propose that this differential behavior is related to the presence of different *Pseudomonas* strains in those syncoms. *Pseudomonas* Root9 negatively correlated with *Acinetobacter* Root1280 in the APO- but not in the BOA-treated *tolerant* syncom at 96 h. In fact, in the BOA-treated samples, this correlation was positive. In the APO-treated *random* syncom, *Pseudomonas* Root329 was positively correlated with *Acinetobacter* Root1280 at 96 h.

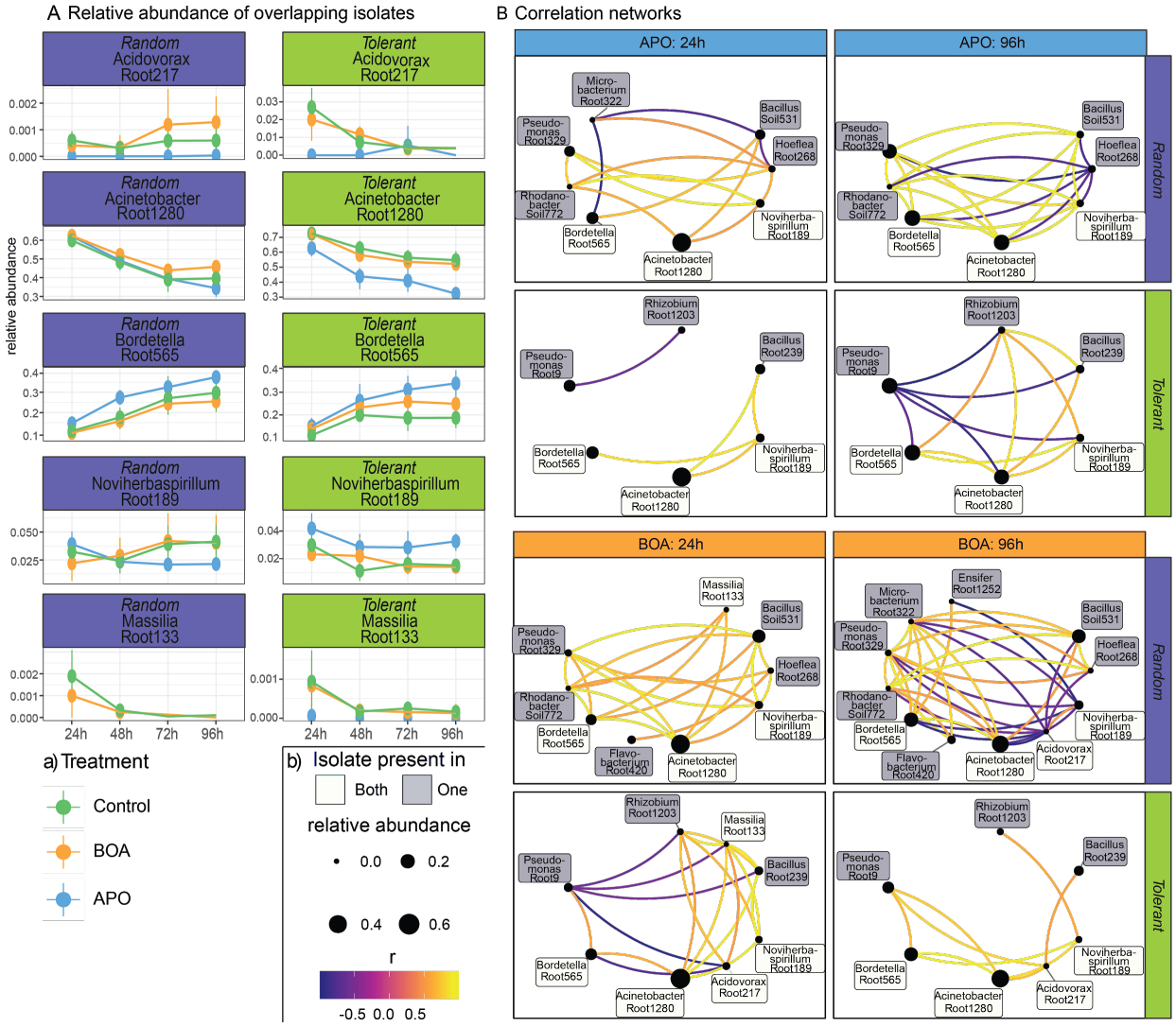

Figure 4. Differential strain interactions in the *random* and *tolerant* syncoms are driven by isolate identity and chemical treatment.

A) Relative abundance of isolates present in both syncoms, over time and by treatment.

B) Pearson's correlations of strain abundances in the *tolerant* and *random* syncoms. Each node represents one isolate; node size reflects relative abundance. Color of the node label indicates if an isolate was a member of both or only one of the syncoms. Each edge indicates a correlation >0.5 between two isolates; edge color indicates the correlation value.

Discussion

Diversity of BX sensitivity in culturable rhizosphere bacteria

In our screen of the *AtRSphere* collection for sensitivity to BX derivatives (Figure 1), we observed broad diversity of growth responses to BX exposure. While some clades were non-responsive to BOA and APO, we observed diverse responses in most clades. APO exerted a strong negative influence on the growth of some isolates. These findings are in line with

previous results showing the antibiotic activity of APO on anaerobic microorganisms [43]. In our study, BOA influenced bacterial growth only marginally compared to APO, similar to what has been described for their effects on fungi and plants. In general, this corroborates the previously suggested relevance of APO, which is more stable than BOA in soil, in BX-mediated plant-environment interactions [14, 16, 21, 23, 44, 45].

However, our data showed that bacterial response to APO was largely isolate-specific and not dictated by phylogenetic relationship. This indicates that even within genera, natural genetic diversity can result in substantial differences in BX sensitivity. Indeed, previous studies reported functional overlap related to responses to plant-derived compounds between isolates from different clades, while not all strains of the same clade shared these functionalities [9, 39]. The broad phylogenetic spectrum of the *AtRSphere* collection prevented the identification of genetic components underlying bacterial response to BOA and APO. However, the strongly differential responses we observed among closely related isolates warrant a more comprehensive analysis of the respective clades in future experiments.

One major advantage of the *AtRSphere* collection is that it was isolated from a non-BX-producing host plant. The soil from which this collection was originally derived (Cologne soil) was collected from an agricultural site, and in absence of a complete record of the field's history, we cannot exclude that there might have been an input of BX in the past. Our findings on the standing diversity of BX tolerance further imply that this diversity is maintained in plant-associated bacteria, also in the absence of a BX-releasing host.

Evaluation of bottom-up design strategy

Others have previously proposed that synthetic communities should be built with a focus on functional features instead of on phylogenetic coverage [30, 46]. We employed a simple, function-guided strategy, compiling syncoms by binning individual isolates based on a specific phenotype and contrasting these binned assemblies to a randomly assembled syncom. The decisive phenotype measured at the level of individual isolates and used for binning them into syncoms was growth upon exposure to APO. The phenotype measured at the community level, variance explained by treatment, was lowest (22%) in the syncom assembled solely from APO-tolerant isolates, indicating that resistance of syncom members leads to overall community resilience. While this approach worked well to create an overall resilient community, the amount of variance explained by treatment was similar in *random* and *sensitive* (~40%) and highest in the *mixed* syncom (75%), indicating that mixing tolerant and sensitive isolates does not necessarily result in a community with intermediate resilience.

Stability of communities *in vitro*

Bacterial communities that assemble *in vitro* are less complex, with respect to the genera they comprise, than those found on and around plant roots yet still contain a considerable number of different isolates in coexistence. One might expect that in an *in vitro* system containing a mixture of isolates, one isolate outgrows the others and reaches very high abundance. This would mean that there are no interactions between the individual isolates and that growth rate is a strong predictor of final abundance. We observed dominance of an isolate in the *sensitive*

community, where *Lysobacter* reached >90% relative abundance. However, upon the addition of BOA we observed that *Flavobacterium* was able to establish itself at >10% relative abundance (corresponding to an eight-fold increase over control). In the *mixed* community, *Bacillus* reached >90% abundance in the BOA and control conditions; however, in the APO treatment, *Bacillus* was strongly reduced in relative abundance, while *Hoeflea* and *Lysobacter* proliferated. In all other syncoms, several isolates reproducibly formed a community, with relative abundances staying within a narrow range across replicates but varying by orders of magnitude between genera.

The growth of an isolate by itself was only poorly correlated with its ability to establish itself as a syncom member or with its relative abundance in a community (Figure 2E). In fact, several isolates that grew poorly on their own reached high relative abundance when grown in communities, possibly indicating facilitation by other members. However, it should be noted that we confirmed a maximum of 15 isolates per syncom by 16S rRNA sequencing.

Chemical stability of isolate interactions

Partial overlap in the communities that arose from the *random* and *tolerant* syncom mixtures allowed us to investigate to which degree the identity of community members influences the interactions between isolates. The *random* and *tolerant* syncoms shared five isolates, three of which were detectable in all treatments and time points. After 96 h, the *random* and *tolerant* communities overlapped in 5 genera, including 3 identical isolates and differing representatives of *Pseudomonas* and *Bacillus*. The identical isolates *Bordetella*, *Acinetobacter*, and *Noviherbaspirillum* positively correlated in both syncoms, indicating that these isolates may form a rather stable network *in vitro*. However, the influence of *Pseudomonas* on this network was negative in the *tolerant* syncom, while the *Pseudomonas* isolate in the *random* syncom was positively correlated with the network formed by *Acinetobacter*, *Bordetella*, and *Noviherbasprillium*. This indicates that the exchange of a single isolate for a closely related isolate from the same genus can have a broad influence on the overall community composition. This supports the view that some community members can facilitate or compete with a larger group of interacting members, i.e., acting as keystones [47], although this ability seems to be variable within a clade.

BX dependent community alterations *in vitro* mimic those described in soil

Our work complements recent research efforts to understand the effect of benzoxazinoids on plant-associated microbiota in soil [17–20, 22]. Ultimately, for *in vitro* syncom systems to be a useful model for plant microbiota research, they should behave similarly to microbiota in soil. BX constitute a prime system to assess this, as the influence of BX release on the root and rhizosphere microbiome has been investigated via mutant studies in different soils [17, 19, 20, 22]. Among the bacterial taxa that were found in different studies, *Flavobacteriales* were observed as depleted in multiple studies. Hu et al [17] found *Flavobacterium* depleted on the roots of BX-exuding plants and the surrounding soils when comparing wildtype and *bx1* mutant plants. Extending these observations, Cadot et al [22] reported that *Flavobacteriaceae* were

consistently depleted on roots of BX-producing plants, independent of soil type and location. Similarly, members of the *Flavobacteriales* family were more abundant on the roots of maize BX-synthesis mutants than on wildtype in another, independent study [20]. In all of the afore-mentioned studies, *Comamonadaceae* were also reported to be depleted on roots of BX-releasing plants when compared to BX-deficient mutants [17, 19, 20, 22].
Our data show that the growth of *Flavobacterium* isolates was only slightly reduced across APO levels, with some isolates displaying mild sensitivity to BOA. However, *Flavobacterium* was significantly depleted from the *random* and *tolerant* syncoms once the community was exposed to APO. *Flavobacterium* was not found in the other two communities. Similarly, *Acidovorax* (*Comamonadaceae*) was found to be reduced in the APO treatment in all syncoms. Thus, even though *in vitro* cultivation strongly differs from soils in physical and chemical parameters and in overall complexity, our study suggests that plant-exudate-mediated effects on soil communities can be recapitulated *in vitro*, highlighting the applicability of such reduced-complexity systems for future studies. In addition, such simplified systems may aid in the identification of microbial isolates that act as community keystones, or hubs, under specific chemical challenges in a short experimental time frame [38]. These data can then be used as basis for the design of host-associated communities that are able to remain stable even in the presence of toxic metabolites, which may increase plant productivity in mixed-cultivation settings.

Methods

Material

Isolate profiling

Individual isolates were pre-cultured in ½ strength TSB medium in 96-Well 2 ml deep-well plates (Semadeni) covered with a Breathe-Easy (Diversified Biotech) membrane until stationary phase for 6 d at 28°C and 180 rpm. Cultures were then resuspended by pipetting up and down 10 times and inoculated into 96-well flat-bottom, transparent cell culture plates (Nunc), containing either solvent control (DMSO), 1 µM APO, 5 µM APO, 10 µM APO, 50 µM APO, 10 µM BOA, 50 µM BOA or 100 µM BOA in ½-strength TSB. Different media were prepared by mixing a stock containing the highest concentration of the respective chemical, with medium containing the solvent at the same concentration (DMSO; 1:20.000). Pipetting was carried out using an Agilent Bravo pipetting robot equipped with a 96-tip head. Plates were stacked without lids, with one empty plate at the top and the bottom of the stack and placed into a BioTek plate stacker connected to a BioTek Synergy2 plate reader. Plates were shaken for 120 s before reading, and absorption (600 nm) was measured in each well. Plates were continuously shaken, measured, and stacked over the course of at least 48 h per replicate. For each replicate, the relative growth per isolate and condition was calculated by dividing the area under the growth curve (x = time in minutes; y = increase in OD600) in the respective condition by the area under the growth curve of the control condition. The experiment was carried out in eight replicates per condition.

Synthetic bacterial communities

Design

To investigate to which degree the overall resilience of a bacterial community to chemical changes is determined by the properties of its individual members, we followed two separate design strategies. In the first strategy, we aimed at creating a diverse community spanning all genera of the strain collection. The *random* community was created by picking one random isolate per genus.
In the second approach, we built communities based on the growth profiles of the individual strains. These communities span a limited number of genera, but the member growth profile is more strictly defined than in the “full” community. One of the reduced representation communities was created from isolates that grew to 75% to 100% of control conditions in 50µM APO (*tolerant*). The other reduced community was assembled from isolates that grew to 0 to 25% of control in 50µM APO (*sensitive*). If there was more than one isolate per genus that fulfilled the condition, we selected one at random. In addition, we compiled one limited representation syncom containing a mix of sensitive and tolerant strains (*mixed*).

Cultivation and sequencing

Individual isolates were pre-cultured in ½-strength TSB medium in 96-Well 2ml deep-well plates covered with a Breathe-Easy membrane (Diversified Biotech) with shaking at 28°C for 6 days until stationary phase, as described previously [39]. Individual cultures were resuspended by pipetting up and down 10 times, and then 100 µL of each culture were mixed with 10 mL ½-strength TSB medium containing solvent at the same concentration as the treatment cultures (1:20.000 DMSO). 100 µL of the mixed culture were used to inoculate 20 mL cultures containing either a solvent control (DMSO), 100 µM BOA, or 50 µM APO in 100 mL Erlenmayer flasks. Flasks were cultured at 28°C, 180 rpm; 1 ml culture was sampled every 24 h. Sampled cultures were centrifuged at 12.000 rpm, the supernatant was discarded and the pellet was stored at -70 °C until further use. DNA was extracted using the DNA PowerSoil kit (Qiagen) following the standard protocol. 16S amplicons were generated according to the Illumina 16S protocol, indexed using Nextera XT dual indexing (Illumina), and pooled per time point for sequencing on a MiSeq (Paired end 300bp, Illumina).

Data analysis

RStudio with R version 4.0.2 was used for data analysis. Reads processed and ASVs were inferred using the dada2 pipeline [48]. Taxonomic assignment of ASVs was done using syncom specific 16SrRNA databases and agglomerated at the genus level. ASVs that could not be assigned were discarded. Scripts used for data analysis are available at https://github.com/nschan/BxSyncomMs. Reads were deposited to ENA, accession number PRJEB42439. The following packages were used:
Tidyverse [49], Broom [50], dada2 [51], DECIPHER [52], DESeq2 [53], emmeans [54], ggforce [55], ggthemes [56], ggtree [57–59], gt [60], igraph [61], MESS [62], multcomp [63], patchwork

[64], phangorn [65, 66], phyloseq [67], vegan [68], wesanderson [69] in combination with some custom functions.

Acknowledgements

The authors gratefully acknowledge support from the Vienna BioCenter Core Facility (VBCF) Molecular Biology Services, especially Dr. Robert Heinen, the VBCF Media Kitchen, the VBCF Sequencing facility and the VBCF High Performance Computing facility. The authors also gratefully acknowledge the Leibniz Supercomputing Centre (LRZ) for funding this project by providing computing time on its Linux-Cluster and Rstudio Server.
The authors thank Eva Knoch and Patrick Hüther for constructive feedback on the manuscript, and Iacopo Gentile and Karina Weiser-Lobao for conducting preliminary experiments and for technical support. The authors also thank Stijn Staepen for help with the *AtRSphere* collection and Paul Schulze-Lefert for helpful discussion.
This work was funded by the Austrian Academy of Sciences (ÖAW) and the European Research Council (ERC) under the European Union's Horizon 2020 research and innovation programme (Grant agreement No. 716823, "FEAR-SAP").

Literature

1. Fitzpatrick CR, Salas-González I, Conway JM, Finkel OM, Gilbert S, Russ D, et al. The Plant Microbiome: From Ecology to Reductionism and Beyond. *Annu Rev Microbiol* 2020.
2. Bulgarelli D, Schlaeppi K, Spaepen S, van Themaat EVL, Schulze-Lefert P. Structure and Functions of the Bacterial Microbiota of Plants. *Annu Rev Plant Biol* **64**: 807–838.
3. Bulgarelli D, Rott M, Schlaeppi K, Ver Loren van Themaat E, Ahmadinejad N, Assenza F, et al. Revealing structure and assembly cues for Arabidopsis root-inhabiting bacterial microbiota. *Nature* 2012; **488**: 91–95.
4. Stringlis IA, Yu K, Feussner K, de Jonge R, Van Bentum S, Van Verk MC, et al. MYB72-dependent coumarin exudation shapes root microbiome assembly to promote plant health. *Proc Natl Acad Sci U S A* 2018.
5. Lebeis SL, Paredes SH, Lundberg DS, Breakfield N, Gehring J, McDonald M, et al. Salicylic acid modulates colonization of the root microbiome by specific bacterial taxa. *Science* 2015; **349**: 860–864.
6. Koprivova A, Schuck S, Jacoby RP, Klinkhammer I, Welter B, Leson L, et al. Root-specific camalexin biosynthesis controls the plant growth-promoting effects of multiple bacterial strains. *Proc Natl Acad Sci U S A* 2019.
7. Voges MJEEE, Bai Y, Schulze-Lefert P, Sattely ES. Plant-derived coumarins shape the composition of an Arabidopsis synthetic root microbiome. *Proc Natl Acad Sci U S A* 2019; **116**: 12558–12565.
8. Jacoby RP, Koprivova A, Kopriva S. Pinpointing secondary metabolites that shape the composition and function of the plant microbiome. *J Exp Bot* 2020.
9. Harbort CJ, Hashimoto M, Inoue H, Niu Y, Guan R, Rombolà AD, et al. Root-Secreted Coumarins and the Microbiota Interact to Improve Iron Nutrition in Arabidopsis. *Cell Host Microbe* 2020; **0**.

10. Frey M, Chomet P, Glawischnig E, Stettner C, Grün S, Winklmair A, et al. Analysis of a chemical plant defense mechanism in grasses. *Science* 1997; **277**: 696–699.
11. Handrick V, Robert CAM, Ahern KR, Zhou S, Machado RAR, Maag D, et al. Biosynthesis of 8-O-Methylated Benzoxazinoid Defense Compounds in Maize. *Plant Cell* 2016; **28**: 1682–1700.
12. Hu L, Mateo P, Ye M, Zhang X, Berset JD, Handrick V, et al. Plant iron acquisition strategy exploited by an insect herbivore. *Science* 2018; **361**: 694–697.
13. Robert CAM, Veyrat N, Glauser G, Marti G, Doyen GR, Villard N, et al. A specialist root herbivore exploits defensive metabolites to locate nutritious tissues. *Ecol Lett* 2011; **14**: 55–64.
14. Venturelli S, Belz RG, Kamper A, Berger A, von Horn K, Wegner A, et al. Plants Release Precursors of Histone Deacetylase Inhibitors to Suppress Growth of Competitors. *Plant Cell* 2015; **27**: 3175–3189.
15. Venturelli S, Petersen S, Langenecker T, Weigel D, Lauer UM, Becker C. Allelochemicals of the phenoxazinone class act at physiologically relevant concentrations. *Plant Signal Behav* 2016; **11**: e1176818.
16. Schulz M, Marocco A, Tabaglio V, Macias FA, Molinillo JMG. Benzoxazinoids in rye allelopathy - from discovery to application in sustainable weed control and organic farming. *J Chem Ecol* 2013; **39**: 154–174.
17. Hu L, Robert CAM, Cadot S, Zhang X, Ye M, Li B, et al. Root exudate metabolites drive plant-soil feedbacks on growth and defense by shaping the rhizosphere microbiota. *Nat Commun* 2018; **9**: 2738.
18. Neal AL, Ahmad S, Gordon-Weeks R, Ton J. Benzoxazinoids in root exudates of maize attract Pseudomonas putida to the rhizosphere. *PLoS One* 2012; **7**: e35498.
19. Kudjordjie EN, Sapkota R, Steffensen SK, Fomsgaard IS, Nicolaisen M. Maize synthesized benzoxazinoids affect the host associated microbiome. *Microbiome* 2019; **7**: 59.

20. Cotton TEA, Pétriacq P, Cameron DD, Meselmani MA, Schwarzenbacher R, Rolfe SA, et al. Metabolic regulation of the maize rhizobiome by benzoxazinoids. *ISME J* 2019.
21. Schandry N, Becker C. Allelopathic Plants: Models for Studying Plant–Interkingdom Interactions. *Trends Plant Sci* 2020; **25**: 176–185.
22. Cadot S, Guan H, Bigalke M, Walser J-C, Jander G, Erb M, et al. Specific and conserved patterns of microbiota-structuring by maize benzoxazinoids in the field. *bioRxiv* . 2020. , 2020.05.03.075135
23. Kumar P, Gagliardo RW, Chilton WS. Soil transformation of wheat and corn metabolites mboa and DIM2BOA into aminophenoxazinones. *J Chem Ecol* 1993; **19**: 2453–2461.
24. Macías FA, Oliveros-Bastidas A, Marín D, Castellano D, Simonet AM, Molinillo JMG. Degradation studies on benzoxazinoids. Soil degradation dynamics of (2R)-2-O-beta-D-glucopyranosyl-4-hydroxy-(2H)- 1,4-benzoxazin-3(4H)-one (DIBOA-Glc) and its degradation products, phytotoxic allelochemicals from Gramineae. *J Agric Food Chem* 2005; **53**: 554–561.
25. Macías FA, Oliveros-Bastidas A, Marín D, Castellano D, Simonet AM, Molinillo JMG. Degradation Studies on Benzoxazinoids. Soil Degradation Dynamics of 2,4-Dihydroxy-7-methoxy-(2 H)-1,4-benzoxazin-3(4 H)-one (DIMBOA) and Its Degradation Products, Phytotoxic Allelochemicals from Gramineae. *J Agric Food Chem* 2004; **52**: 6402–6413.
26. Anzai K, Isono K, Okuma K, Suzuki S. The new antibiotics, questiomycins A and B. *J Antibiot* 1960; **13**: 125–132.
27. Imai S, Shimazu A, Furihata K, Furihata K, Hayakawa Y, Seto H. Isolation and structure of a new phenoxazine antibiotic, exfoliazone, produced by Streptomyces exfoliatus. *J Antibiot* 1990; **43**: 1606–1607.
28. Cheng C, Othman EM, Fekete A, Krischke M, Stopper H, Edrada-Ebel R, et al. Strepoxazine A, a new cytotoxic phenoxazin from the marine sponge-derived bacterium Streptomyces sp. SBT345. *Tetrahedron Lett* 2016; **57**: 4196–4199.

29. Belz RG, Hurle K. Differential exudation of two benzoxazinoids--one of the determining factors for seedling allelopathy of Triticeae species. *J Agric Food Chem* 2005; **53**: 250–261.
30. Vorholt JA, Vogel C, Carlström CI, Müller DB. Establishing Causality: Opportunities of Synthetic Communities for Plant Microbiome Research. *Cell Host Microbe* 2017; **22**: 142–155.
31. Herrera Paredes S, Gao T, Law TF, Finkel OM, Mucyn T, Teixeira PJPL, et al. Design of synthetic bacterial communities for predictable plant phenotypes. *PLoS Biol* 2018; **16**: e2003962.
32. Vrancken G, Gregory AC, Huys GRB, Faust K, Raes J. Synthetic ecology of the human gut microbiota. *Nat Rev Microbiol* 2019; **17**: 754–763.
33. De Roy K, Marzorati M, Van den Abbeele P, Van de Wiele T, Boon N. Synthetic microbial ecosystems: an exciting tool to understand and apply microbial communities. *Environ Microbiol* 2014; **16**: 1472–1481.
34. Finkel OM, Salas-González I, Castrillo G, Conway JM, Law TF, Teixeira PJPL, et al. A single bacterial genus maintains root growth in a complex microbiome. *Nature* 2020.
35. Liu Y-X, Qin Y, Bai Y. Reductionist synthetic community approaches in root microbiome research. *Curr Opin Microbiol* 2019; **49**: 97–102.
36. Trivedi P, Leach JE, Tringe SG, Sa T, Singh BK. Plant-microbiome interactions: from community assembly to plant health. *Nat Rev Microbiol* 2020.
37. Bodenhausen N, Bortfeld-Miller M, Ackermann M, Vorholt JA. A synthetic community approach reveals plant genotypes affecting the phyllosphere microbiota. *PLoS Genet* 2014; **10**: e1004283.
38. Carlström CI, Field CM, Bortfeld-Miller M, Müller B, Sunagawa S, Vorholt JA. Synthetic microbiota reveal priority effects and keystone strains in the Arabidopsis phyllosphere. *Nat Ecol Evol* 2019; **3**: 1445–1454.
39. Bai Y, Müller DB, Srinivas G, Garrido-Oter R, Potthoff E, Rott M, et al. Functional overlap of

the Arabidopsis leaf and root microbiota. *Nature* 2015; 1–19.

40. Li L, Abou-Samra E, Ning Z, Zhang X, Mayne J, Wang J, et al. An in vitro model maintaining taxon-specific functional activities of the gut microbiome. *Nat Commun* 2019; **10**: 4146.
41. Dessaux Y, Grandclément C, Faure D. Engineering the Rhizosphere. *Trends Plant Sci* 2016; **21**: 266–278.
42. Ke J, Wang B, Yoshikuni Y. Microbiome Engineering: Synthetic Biology of Plant-Associated Microbiomes in Sustainable Agriculture. *Trends Biotechnol* 2020.
43. Atwal AS, Teather RM, Liss SN, Collins FW. Antimicrobial activity of 2-aminophenoxazin-3-one under anaerobic conditions. *Can J Microbiol* 1992; **38**: 1084–1088.
44. Schütz V, Bigler L, Girel S, Laschke L, Sicker D, Schulz M. Conversions of Benzoxazinoids and Downstream Metabolites by Soil Microorganisms. *Frontiers in Ecology and Evolution* 2019; **7**: 238.
45. Voloshchuk N, Schütz V, Laschke L, Gryganskyi AP, Schulz M. The Trichoderma viride F-00612 consortium tolerates 2-amino-3H-phenoxazin-3-one and degrades nitrated benzo[d]oxazol-2(3H)-one. *Chemoecology* 2020.
46. Lemanceau P, Blouin M, Muller D, Moënne-Loccoz Y. Let the Core Microbiota Be Functional. *Trends Plant Sci* 2017; **22**: 583–595.
47. Banerjee S, Schlaeppi K, van der Heijden MGA. Keystone taxa as drivers of microbiome structure and functioning. *Nat Rev Microbiol* 2018; **16**: 567–576.
48. Callahan BJ, Sankaran K, Fukuyama JA, McMurdie PJ, Holmes SP. Bioconductor Workflow for Microbiome Data Analysis: from raw reads to community analyses. *F1000Res* 2016; **5**: 1492.
49. Wickham H, Averick M, Bryan J, Chang W, McGowan L, François R, et al. Welcome to the Tidyverse. *JOSS* 2019; **4**: 1686.
50. Robinson D, Hayes A, Couch S. Broom: Convert statistical objects into tidy tibbles. 2019.

51. Callahan BJ, McMurdie PJ, Rosen MJ, Han AW, Johnson AJA, Holmes SP. DADA2: High-resolution sample inference from Illumina amplicon data. *Nat Methods* 2016; **13**: 581–583.
52. Wright ES. Using DECIPHER v2. 0 to analyze big biological sequence data in R. *R J* 2016; **8**.
53. Love MI, Huber W, Anders S. Moderated estimation of fold change and dispersion for RNA-seq data with DESeq2. *Genome Biol* 2014; **15**: 550.
54. Lenth R, Singmann H, Love J, Buerkner P, Herve M. emmeans: Estimated Marginal Means, aka Least-Squares Means (Version 1.3. 4). 2019.
55. Pedersen TL. ggforce: Accelerating 'ggplot2'. 2020.
56. Arnold JB. ggthemes: Extra Themes, Scales and Geoms for 'ggplot2'. 2019.
57. Yu G, Smith D, Zhu H, Guan Y, Lam TT-Y. ggtree: an R package for visualization and annotation of phylogenetic trees with their covariates and other associated data. *Methods in Ecology and Evolution* . 2017. , **8**: 28–36
58. Yu G, Lam TT-Y, Zhu H, Guan Y. Two methods for mapping and visualizing associated data on phylogeny using ggtree. *Molecular Biology and Evolution* . 2018. , **35**: 3041–3043
59. Yu G. Using ggtree to Visualize Data on Tree-Like Structures. *Current Protocols in Bioinformatics* . 2020. , **69**: e96
60. Iannone R, Cheng J, Schloerke B. gt: Easily Create Presentation-Ready Display Tables. 2019. R package version 0.1. 0.
61. Csardi G, Nepusz T. The igraph software package for complex network research. *InterJournal* . 2006. , **Complex Systems**: 1695
62. Ekstrøm C. MESS: Miscellaneous Esoteric Statistical Scripts. 2016.
63. Hothorn T, Bretz F, Westfall P. Simultaneous inference in general parametric models. *Biom J* 2008; **50**: 346–363.
64. Pedersen TL. patchwork: The Composer of Plots. 2020.
65. Schliep KP. phangorn: phylogenetic analysis in R. *Bioinformatics* . 2011. , **27**: 592–593

66. Schliep, Klaus, Potts, J. A, Morrison, A. D, et al. Intertwining phylogenetic trees and networks. *Methods in Ecology and Evolution* . 2017. , **8**: 1212–1220
67. McMurdie PJ, Holmes S. phyloseq: an R package for reproducible interactive analysis and graphics of microbiome census data. *PLoS One* 2013; **8**: e61217.
68. Oksanen J, Blanchet FG, Friendly M, Kindt R, Legendre P, McGlinn D, et al. vegan: Community Ecology Package. 2019.
69. Ram K, Wickham H. wesanderson: A Wes Anderson Palette Generator. 2018.

Supplemental Figures

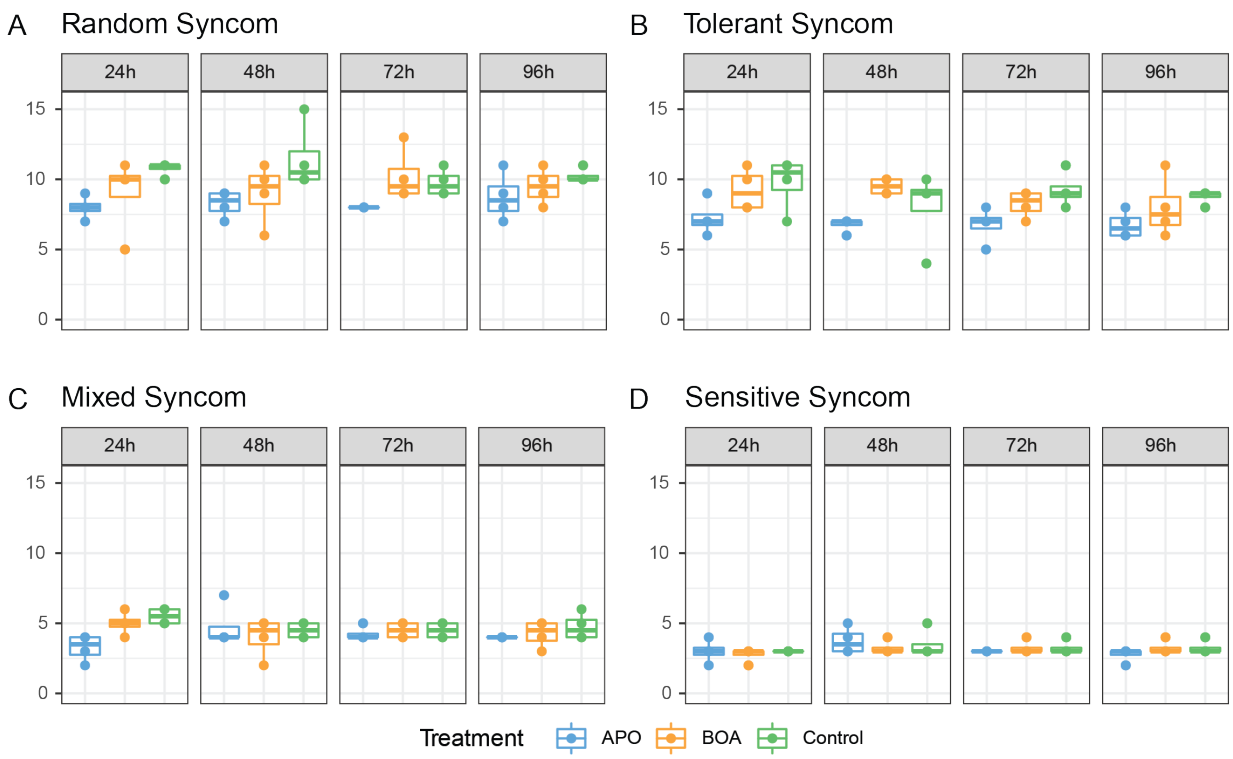

Figure S1. Observed alpha diversity.
The number of observed bacterial genera of the samples belonging to the four different syncoms **(A-D)** is shown for each time point (facet) and treatment (color). Each sample is plotted as a dot, and box-and-whisker plots show the summary statistics for each treatment / time point combination.

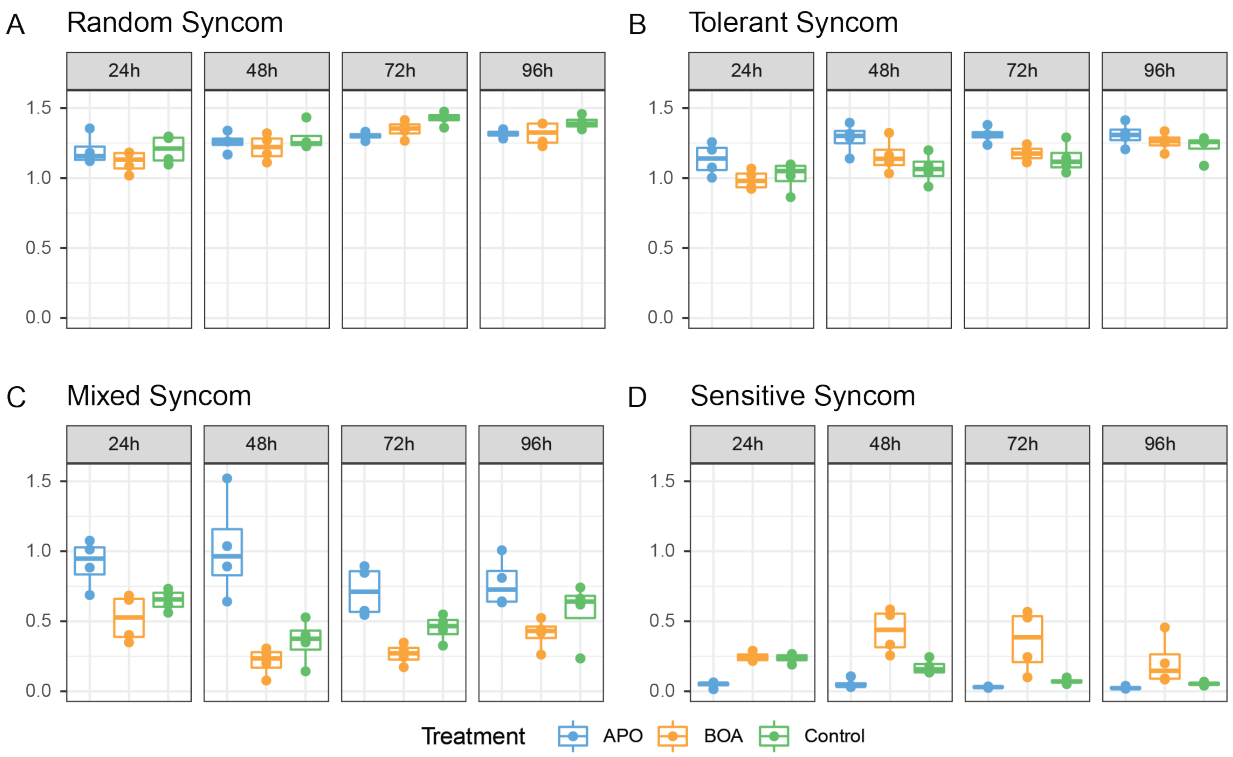

Figure S2: Shannon diversity indices of the synthetic communities.
The Shannon indices of the samples belonging to the four different syncoms **(A-D)** is shown for each time point (facet) and treatment (color). Each sample is plotted as a dot, and box-and-whisker plots show the summary statistics for each treatment / time point combination.

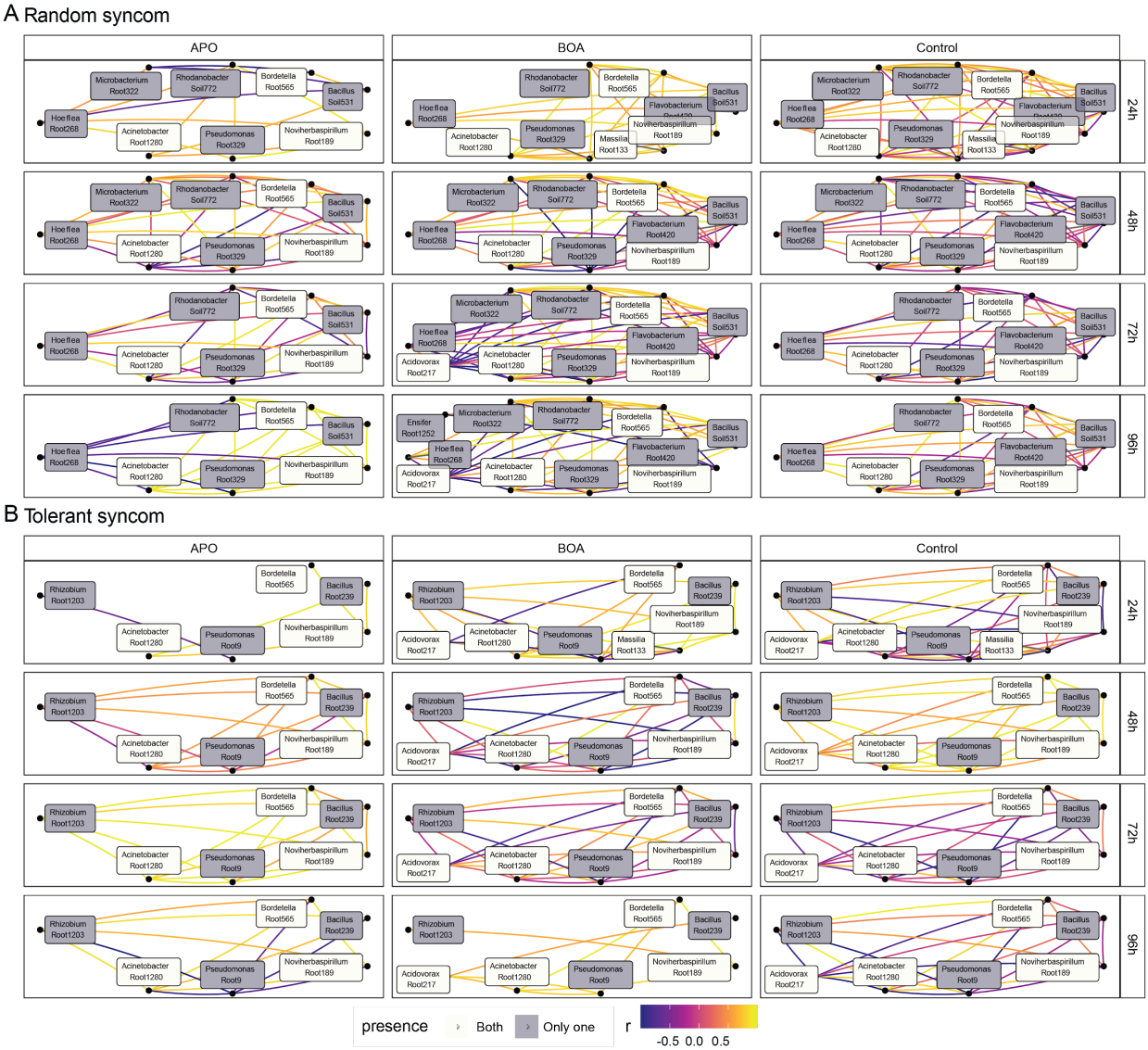

Figure S3: Network correlations.
Networks of isolate Pearson correlations in the *random* (A) and *tolerant* (B) syncom. Each individual plot shows correlations between isolates for one time point and treatment combination. The color of each edge indicates the strength, and sign of the correlation (blue: negative correlation; yellow: positive) and each node represents one isolate. The background color of the node label indicates whether an isolate was part of both communities (white) or only included in one (gray). Only correlations that had an absolute r > 0.5 were included.